Electrostatically Self-assembled Multilayers of Novel Symmetrical Rigid-Rod Polyanionic and Polycationic Polythiophenes on ITO/Glass and Gold Electrodes

Gianni Zotti,* Sandro Zecchin, Gilberto Schiavon, and Barbara Vercelli

Istituto CNR per l'Energetica e le Interfasi, C.o Stati Uniti 4, 35127 Padova, Italy

Anna Berlin*

Istituto CNR di Scienze e Tecnologie Molecolari, via C. Golgi 19, 20133 Milano, Italy

William Porzio

Istituto CNR per lo Studio delle Macromolecole, via E. Bassini 15, 20133 Milano, Italy

Received November 13, 2003. Revised Manuscript Received March 30, 2004

Anodic coupling of 4,4-bis-butanesulfonate cyclopentadithiophene occurs in acetonitrile after the addition of 1:1 $HClO_4$ to yield water-soluble polyanionic poly(1). 4,4-Bis-hexyltrimethylammonium cyclopentadithiophene is polymerized in acetonitrile to acetonitrile-soluble polycationic poly(2) which is converted to the water-soluble hydroxide form by anion exchange. These novel water-soluble polythiophenes, characterized by a rigid-rod symmetrical shape of the chain, display a high conjugation length (λ_{max} = 560−575 nm) and a good solubility in water (>10 gL^{-1}). MALDI and UV−vis spectroscopy assign these polymers a degree of polymerization of 5−6. The polymers form stable monolayers (storing a redox charge of 10 $\mu C\ cm^{-2}$) on ITO/glass and gold electrodes. Subsequent electrostatic self-assembly (ESA) of poly(1) and poly(2), both between them and each with a non-electroactive polycation or polyanion, proceeds with a linear growth rate monitored by cyclic voltammetry (10 $\mu C\ cm^{-2}$ $bilayer^{-1}$) and UV−vis spectroscopy. No effect of ionic strength was observed in contrast with ESA of conventional polyionic polymers. IRRAS and XRD analysis of the multilayers agree with a regular disposition of the polythiophene chains in the layers.

1. Introduction

Over the past decade the layer-by-layer electrostatic adsorption technique introduced by Decher and Hong[1] has been particularly considered as a way to prepare thin polymer films. This self-assembly method involves the sequential adsorption of polyelectrolytes from dilute solution onto an oppositely charged substrate, leading to charge reversal on the surface. The simplicity of the method makes layer-by-layer self-assembly applicable to a wide variety of polyelectrolytes, including, for example, biopolymers and polyelectrolytes functionalized with nonlinear optical groups,[2,3] and attractive for a number of potential applications such as electro-optic devices and sensors.[4,5] The formation of multilayer films by this electrostatic self-assembly (ESA) has been recently reviewed.[6]

Concerning polyconjugated conducting polymers, several papers have been published.[7] In particular, the literature reports on poly(3-carboxymethylthiophene) in alternation with polycationic polyammonium layers,[8,9] polyaniline sulfonate and polyallylamine,[10] polyaniline sulfonate or poly(phenylene vinylene) polymer bilayers,[11] poly(phenylene)s with sulfonate and quaternary ammonium functionalizations,[12] polypyrrole,[13,14] and polyaniline;[15] poly-3-(3′-thienyloxy)propanesulfonate/poly-3-(3′-thienyloxy)propyltriethylammonium[16] and poly-(3-octanic acid)thiophene/poly(3-hexylammonium thiophene);[17] diammonium-sexithiophene and polystyrene-

* Authors to whom correspondence should be addressed. Dr. Gianni Zotti, Istituto CNR per l'Energetica e le Interfasi, C.o Stati Uniti 4, 35127 Padova, Italy. Tel.: (39)049-829-5868. Fax: (39)049-829-5853. E-mail: g.zotti@ieni.cnr.it.

(1) (a) Decher, G.; Hong, J. *Makromol. Chem. Macromol. Symp.* **1991**,*46*, 321; (b) Decher, G.; Hong, J. *Ber. Bunsen-Ges. Phys. Chem.* **1991**, *95*, 1430. (c) Decher, G. *Science* **1997**, *277*, 1232.

(2) Caruso, F.; Schuler, C. *Langmuir* **2000**, *16*, 9595.

(3) Lee, S. H.; Balasubramanian, S.; Kim, D. Y.; Viswanathan, N. K.; Bian, S.; Kumar, J.; Tripathy, S. K. *Macromolecules* **2000**, *33*, 6534.

(4) Donath, E.; Sukhorukov, G. B.; Caruso, F.; Davis, S. A.; Mohwald, H. *Angew. Chem, Int. Ed.* **1998**, *37*, 2202.

(5) Dai, J.; Jensen, A. W.; Mohanty, D. K.; Erndt, J.; Bruening, M. J. *Langmuir* **2001**, *17*, 931.

(6) Bertrand, P.; Jonas, A.; Laschewsky, A.; Legras, R. *Macromol. Rapid. Commun.* **2000**, *21*, 319.

(7) Berlin, A.; Zotti, G. *Macromol. Rapid Commun.* **2000**, *21*, 301 and references therein.

(8) Kawai, T.; Yamaue, T.; Tada, K.; Onoda, M.; Jin, S. H.; Choi, S. K.; Yoshino, K. *Jpn. J. Appl. Phys.* **1996**, *35*, L741.

(9) Ferreira, M.; Cheung, J. H.; Rubner, M. F. *Thin Solid Films* **1994**, *244*, 806.

(10) Kellogg, G. J.; Mayers, A. M.; Stockton, W. B.; Ferreira, M.; Rubner, M. F.; Satija, S. K. *Langmuir* **1996**, *12*, 5109.

(11) Ho, P. K. H.; Graustrom, M.; Friend, R. H.; Greenham, N. C. *Adv. Mater.* **1998**, *10*, 769.

(12) Baur, J. W.; Kim, S.; Balanda, P. B.; Reynolds, J. R.; Rubner, M. F. *Adv. Mater.* **1998**, *10*, 1452.

(13) (a) Cheung, J. H.; Fou, A. C.; Rubner, M. F. *Thin Solid Films* **1994**, *244*, 985. (b) Fou, A. C.; Rubner, M. F. *Macromolecules* **1995**, *28*, 7115.

(14) Ram, M. K.; Adami, M.; Faraci, P.; Nicolini, C. *Polymer* **2000**, *41*, 7499.

10.1021/cm0351644 CCC: $27.50
Published on Web 05/08/2004

Chart 1

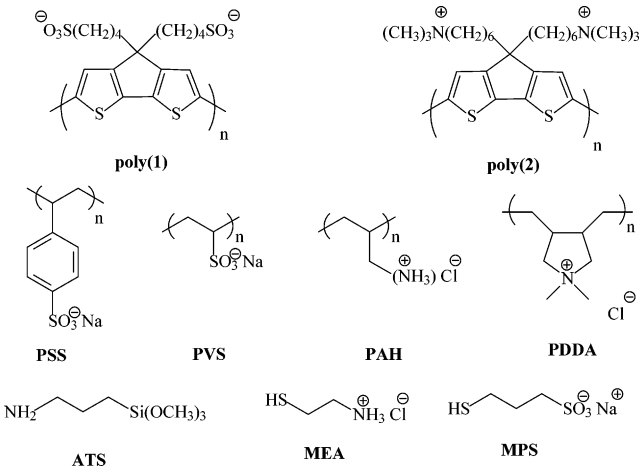

sulfonate;[18] poly-3-(3′-thienyloxy)propanephosphonate[19] and poly(phenylene ethynilene) phosphonate[20] with polyammonium.

Multilayers based on polyconjugated polymers in the conducting state have been recently prepared from a water-soluble poly(3,4-ethylenedioxythiophene) sulfonate in alternation with polyallylamine.[21]

We have previously reported the production of soluble and conducting polythiophenes from anodic coupling of tetrabutylammonium 4-(4*H*-cyclopentadithien-4-yl)butanesulfonate[22] and {6-(4-hexyl-4*H*-cyclopenta[2,1-b:3,4-b′]dithiophen-4yl)hexyl}trimethylammonium perchlorate.[23] These cyclopentadithiophene-based polymers were used for the alternate layering of polyanions and polycations.[24]

Here, we consider the analogous polymers with symmetrical alkylsulfonate and alkylammonium disubstitution at the 4 positions and their ESA between them and with other conventional polyions (Chart 1) on indium−tin−oxide/glass and gold electrodes. It is expected that these rigid-rod symmetrical molecules arrange in layers with unprecedented regularity. The resulting order would increase the anisotropy of the electronic (optical and conductive) properties of the polyconjugated chains. Moreover, their high charge density is expected to produce very stable layers.[25] The formation of mono- and multilayers has been monitored by cyclic voltammetry CV and UV−vis spectroscopy and supported by IRRAS, XRD, and AFM analysis.

2. Experimental Section

2.1. Chemicals and Reagents. All melting points are uncorrected. All reactions of air- and water-sensitive materials were performed under nitrogen. Air- and water-sensitive solutions were transferred with double-ended needles. The solvents used in the reactions were dried by conventional methods and freshly distilled under nitrogen. Acetonitrile was reagent grade (Uvasol, Merck) with a water content <0.01%. The supporting electrolyte tetrabutylammonium perchlorate (Bu_4NClO_4) was previously dried under vacuum at 70 °C. The polycations poly(allylamine hydrochloride) (PAH) (M_w = 15000) and poly(diallyldimethylammonium chloride) (PDDA) (M_w = 250000−400000) and the polyanions poly(sodium-*p*-styrenesulfonate) (PSS) (M_w = 100000) and poly(sodium-vinylsulfonate) (PVS) (M_w = 250000) were purchased from Aldrich and used as received. 3-Aminopropyltrimethoxysilane (ATS) was purchased from Fluka. 3-Mercapto-1-propanesulfonic acid sodium salt (MPS) and mercaptoethylamine hydrochloride (MEA) for gold substrate functionalization were also from Aldrich.

H^+-exchange resin (Dowex HCR−W2) and OH^--exchange resin (MTO-Dowex SBR LCNG) were purchased from Supelco.

^1H and ^{13}C NMR spectra were recorded on a Bruker FT 300 (300 MHz for ^1H); chemical shifts value are given in ppm.

The monomers 4[4-(4-sulfobutyl)-4*H*-cyclopenta[2,1-b:3,4-b′]-dithiophen-4-yl]butane sulfonic acid dilithium salt (**1**) and {6-[4-(6-trimethylammonium-hexyl)- 4*H*-cyclopenta[2,1-b:3,4-b′]-dithiophen-4-yl]-hexyl}trimethylammonium diperchorate (**2**) were synthesized as described below starting from 4*H*-cyclopenta[2,1-b:3,4-b′]dithiophene (CPDT).[26] In particular, **2** was synthesized as the dibromide and transformed into the perchlorate by anion exchange and titration of the resulting hydroxide with perchloric acid.

4[4-(4-Sulfobutyl)-4*H*-cyclopenta[2,1-b:3,4-b′]dithiophen-4-yl]butane Sulfonic Acid Dilithium Salt (1). BuLi (1.6 M in hexane, 1.05 mL, 1.68 mmol) was added dropwise to a stirred solution of CPDT (300 mg, 1.68 mmol) in THF (10 mL) maintained at 0 °C. After 1 h of stirring at room temperature, the reaction mixture was cooled to 0 °C and a solution of 1,4-butanesultone (229 mg, 1.68 mmol) in THF (3 mL) was added dropwise, and the reaction mixture was stirred at room temperature for 1.5 h. A second portion of BuLi (1.6 M in hexane, 1.05 mL, 1.68 mmol) was added at 0 °C, the reaction mixture stirred for 1 h at room temperature, and a solution of 1,4-butanesultone (229 mg, 1.68 mmol) in THF (3 mL) was added dropwise at 0 °C and the resulting mixture stirred 1.5 h at room temperature. The solid precipitated was filterd and dissolved in water. The resulting solution was extracted with ether and evaporated at reduced pressure to give the title compound as a white solid (350 mg, 52% yield), mp > 250 °C. Anal. Calcd for $C_{17}H_{20}Li_2O_6S_2$: C, 51.26; H, 5.02%. Found: C, 51.12; H, 4.97%. ^1H NMR (D_2O): δ 0.97(m, 4H), 1.52 (m, 4H), 2.01 (m, 4H), 2.73 (m, 4H), 7.15 (d, 2H), 7.32 (d, 2H).

4,4-Bis(6-bromohexyl)-4*H*-cyclopenta[2,1-b:3,4-b′]-dithiophene (3). BuLi (1.6 M in hexane, 1.10 mL, 1.76 mmol) was added dropwise to a stirred solution of CPDT (307 mg, 1.72 mmol) in THF (10 mL), keeping the temperature at 0 °C. After reaching room temperature, the solution was stirred for 1 h and then added dropwise to a solution of 1,6-dibromohexane (1.69 g, 6.92 mmol) in THF (10 mL), keeping the temperature at −30 °C. After 1.5 h of stirring at room temperature, the reaction mixture was cooled to 0 °C and BuLi (1.6 M in hexane, 1.25 mL. 2.00 mol) was added dropwise. After 1.5 h of stirring at room temperature, the reaction mixture was

(15) (a) Cheung, J. H.; Stockton, W. B.; Rubner, M. F. *Macromolecules* **1997**, *30*, 2712. (b) Stockton, W. B.; Rubner, M. F. *Macromolecules* **1997**, *30*, 2717. (c) Ram, M. K.; Salemo, M.; Adami, M.; Faraci, P.; Nicolini, C. *Langmuir* **1999**, *15*, 1252.

(16) (a) Lukkari, J.; Salomaki, M.; Viinikanoja, A.; Aaritalo, T.; Paukkunen, J.; Kocharova, N.; Kankare, J. *J. Am. Chem. Soc.* **2001**, *123*, 6083. (b) Lukkari, J.; Salomaki, M.; Aaritalo, T.; Loikas, K.; Laiho, T.; Kankare, J. *Langmuir* **2002**, *18*, 8496.

(17) Zhai, L.; McCullough, R. D. *Adv. Mater.* **2002**, *14*, 901.

(18) Locklin, J.; Youk, J. H.; Xia, C.; Park, M. K.; Fan, X.; Advincula, R. C. *Langmuir* **2002,** *18*, 877.

(19) Viinikanoja, A. ; Lukkari, J.; Aaritalo, T.; Laiho, T.; Kankare, J. *Langmuir* **2003**, *19*, 2768.

(20) Pinto, M. R.; Kristal, B. M.; Schanze, K. S. *Langmuir* **2003**, *19*, 6523.

(21) Cutler, C.; Bougettaya, M.; Reynolds, J. R. *Adv. Mater.* **2002**, *9*, 684.

(22) Zotti, G.; Zecchin, S.; Schiavon, G.; Berlin, A.; Pagani, G.; Canavesi, A. *Chem. Mater.* **1997**, *9*, 2940.

(23) Zotti, G.; Zecchin, S.; Schiavon, G.; Berlin, A. *Macromolecules* **2001**, *34*, 3889.

(24) Zotti, G.; Zecchin, S.; Berlin, A.; Schiavon, G.; Giro, G. *Chem. Mater.* **2001**, *13*, 43.

(25) Hoogeveen, N. G.; Cohen Stuart, M. A.; Fleeer, G. J. *Langmuir* **1996**, *12*, 3675.

(26) Benincori, T.; Brenna, E.; Sannicolo, F.; Trimarco, L.; Moro, G.; Pitea, D.; Pilati, T.; Zerbi, G.; Zotti, G. *J. Chem. Soc., Chem. Commun*. **1995,** 881 and ref. therein; Benincori, T.; Bongiovanni, C.; Botta, C.; Cerullo, G.; Lanzani, G.; Mura, A.; Rossi, L.; Sannicolo, F.; Tubino, R. *Phys. Rev. B* **1998,** *58*, 9082.

poured into water and extracted with ether. The organic phase was dried (Na_2SO_4) and the solvent evaporated. Flash chromatography (silica gel, petrol ether) of the residue afforded the title compound as an oil (862 mg, 50% yield). Anal. Calcd for $C_{21}H_{28}Br_2S_2$: C, 50.00; H, 5.56%. Found: C, 49.91; H, 5.37%. ^{1}H NMR ($CDCl_3$): δ 0.90 (m, 4H), 1.14 (m, 4 H), 1.25 (m, 4H), 1.72 (m, 4H), 1.83 (m, 4H), 3.32 (t, 4H), 6.91 (d, 2H), 7.15 (d, 2H).

{6-[4-(6-Trimethylammonium-hexyl)-4*H*-cyclopenta-[2,1-b:3,4-b′]dithiophen-4-yl)hexyl}trimethylammonium Dibromide (2a). A mixture of **3** (209 mg, 8.40 mmol) and trimethylamine (4.2 M in ethanol, 8.4 mmol) was stirred for 72 h at room temperature. After removal of the solvent, the residue was repetitiously washed with petrol ether, to remove traces of starting compound, and dried to give the title compound as a white solid (207 mg, 79% yield). Anal. Calcd for $C_{27}H_{46}Br_2N_2S_2$: C, 52.12; H, 7.39; N, 4.50%. Found: C, 51.99; H, 7.32; N, 4.39%. ^{1}H NMR (CD_3CN): δ 0.85 (m, 4H), 1.16 (m, 8H), 1.55 (m, 4H), 1.94 (m, 4H), 3.00 (s, 18H), 3.17 (m, 4H), 7.06 (d, 2H), 7.28 (d, 2H). ^{13}C NMR (CD_3CN): δ 23.16, 24.76, 26.25, 29.63, 38.00, 53.76, 54.12, 67.26, 122.98, 126.28, 137.20, 159.12.

2.2. Method for Monolayer and Multilayer Deposition. ITO/glass electrodes were 1 × 4 cm^2 indium−tin−oxide one-side coated glass sheets (20 Ω sq^{-1}, Balzers, Liechtenstein). The ITO microstructure consists of grains ca. 100-nm long and 3-nm high (average). The ITO/glass electrodes were cleaned with acetone and dried prior to use. SIMS has shown that the glass side of the ITO/glass sheet is covered with a thin and non-electroactive yet homogeneous ITO film (5 vs 100 nm of the ITO side) so that the layers are formed in any case on ITO surfaces and on both sides of the sheet.

Monolayers were built on the ITO/glass electrode as such or after monolayer silanization with ATS. In the latter case the clean ITO/glass substrate was immersed for 1 h in 5% ATS solution in nitrogen-degassed dry toluene and then washed with dry toluene and dried.[1]

Gold electrodes were 1 × 4 cm^2 sheets. They were treated for 1 min with mixed chromic acid ($K_2Cr_2O_7$ in 96% H_2SO_4), then carefully washed with Milli-Q water, and dried. The gold surface was then functionalized by immersion for 1 h in an ethanol solution of MPS (0.001 M)[27] or MEA (5% ww),[28] creating a uniformly charged (negative for MPS and positive for MEA) substrate surface.

The buildup of the multilayers was performed according to the methodology introduced by Decher and co-workers,[1,29] that is, by dipping the electrodes alternatively into the solutions of the two polymers. Immersion times were 5 min. After each immersion step the substrate was carefully washed with Milli-Q water (two steps) and dried in air.

The layer buildup was monitored by cyclic voltammetry and UV−vis spectroscopy. For the latter the absorbance data are given as measured, that is, for the sum of the sides of the electrode.

The concentration of the polyion solutions were kept low ($\leq 10^{-2}$ M) to avoid the formation of films thicker by charge shielding or possible coiling of polymer chains.[30,31] The non-electroactive polyions were used as 10^{-2} M water solutions. With the only exception of PDDA they were brought to pH = 3 by addition of $HClO_4$. The thiophene-based polyions (ca 10^{-3} M) were produced and used as described below.

2.3. Apparatus and Procedure. Experiments were performed at 25° C under nitrogen in three electrode cells. Unless otherwise stated, the supporting electrolyte was tetrabutylammonium perchlorate (Bu_4NClO_4) 0.1 M in acetonitrile. The counter electrode was platinum; reference electrode was a silver/0.1 M silver perchlorate in acetonitrile (0.34 V vs SCE). A platinum sheet (15 cm^2) was used in preparative electrolyses. The voltammetric apparatus (AMEL, Italy) included a 551 potentiostat modulated by a 568 programmable function generator and coupled to a 731 digital integrator.

UV−vis spectra were taken with a Perkin-Elmer Lambda 15 spectrometer. MAtrix-assisted Laser Desorption Ionization (MALDI) mass spectra were taken on a Reflex TOF spectrometer (Bruker) operating in the positive reflection mode, using 2,5-dihydroxybenzoic acid as the matrix.

Conductivity measurements were performed on films cast on a glass substrate. A Kuliche-Soffa four-probe head (U.K.) with a Keithley 220 programmable current source and a Keithley 195A digital multimeter were used.

FTIR spectroscopy was performed using a FTIR spectrometer (Perkin-Elmer 2000). InfraRed Reflection Absorption Spectroscopy (IRRAS) spectra of the layers were taken with a grazing incidence reflection unit (Specac). All spectra were recorded with 2-cm^{-1} resolution at an angle of incidence of 80° relative to the surface normal. Ten cycles were run for each spectrum and weighted subtraction of the background at the end of the series of measurements was applied. No gas purging of the chamber was necessary.

Atomic force microscopy (AFM) was performed in noncontact mode in air at room temperature using a DME DS 95-200 Dualscope STM equipped with non-contact mode silicon tips.

X-ray diffraction (XRD) experiments on multilayers were performed at room temperature using a Siemens D-500 diffractometer equipped with a graphite monochromator and Soller slits before and after the sample in Bragg−Brentano geometry. 1° aperture windows and 0.05° receiving slits were adopted; Cu Kα radiation at the power of 40 kV × 40 mA was used. This geometry permits the evidence of interlayer spacings normal to the substrate. Five samples for each multilayer type were examined.

Theoretical evaluation of coverage degree was performed by molecular mechanics calculations using MATSTUDIO program.[32]

2.4. Synthesis of Poly(1) Solution. Bulk oxidized poly(1) is deposited at a 2 × 5 cm^2 platinum sheet electrode by potentiostatic oxidation at 0.7 V of a ca. 2 × 10^{-3} M solution of **1** (25 mg, 0.054 mmol) in acetonitrile + 0.1 M Bu_4NClO_4 (25 mL) after addition of $HClO_4$ in a 2:1 ratio to the monomer. After the passage of 2.0 F mol^{-1} the deposit is washed in acetonitrile and dried. It is then dissolved in water to give a blue-green solution, which is filtered from some insoluble residue, passed through H^+-exchange resin to produce the acidic form alone and then brought to 25 mL (ca 0.1 wt % or ca. 10^{-3} M of repeat units). The doped polymer solution is dedoped with a 10-fold excess of hydrazine.

2.5. Synthesis of Poly(2) Solution. Bulk oxidized poly(2) is produced in solution by potentiostatic oxidation of a ca. 2 × 10^{-3} M solution of **2** (30 mg) in acetonitrile + 0.1 M $NaClO_4$ (25 mL) at 0.7 V (with the passage of 2.1 F mol^{-1}) followed by solvent evaporation and extraction of sodium perchlorate, residual monomer, and side products with hot water. The dark blue poly(2)−ClO_4 (25 mg) is dissolved in 10 mL of 1:1 vv acetonitrile:water and the dark blue solution is passed through OH^--exchange resin to produce the hydroxide form poly(2)−OH and then brought to 25 mL of water (ca 0.1 wt % or ca. 10^{-3} M of repeat units). The poly(2)−OH solution is obtained in the undoped form.

3. Results and Discussion

3.1. Monomers Synthesis. The synthetic access to monomers **1** and **2** is reported in Scheme 1. Compound **1** was prepared in a one-pot reaction of 4*H*-cyclopenta-[2,1-b:3,4-b′]dithiophene (CPDT) first with an equimolar amount of BuLi followed by an equimolar amount of 1,4-

(27) Laurent, D.; Schlenoff, J. B. *Langmuir* **1997**, *13*, 1552.
(28) Kovtyukhova, N. I.; Martin, B. R.; Mbbindyo, J. K. N.; Smith, P. A.; Razavi, B.; Mayer, T. S.; Mallouk, T. E. *J. Phys. Chem. B* **2001**, *105*, 8762.
(29) Lvov, Y.; Decher, G.; Mohwald, H. *Langmuir* **1993**, *9*, 481.
(30) Lowack, K.; Helm, C. A. *Macromolecules* **1998**, *31*, 823.
(31) Schlenoff, J. B.; Ly, H.; Li, M. *J. Am. Chem. Soc.* **1998**, *120*, 7626.
(32) MATERIALS STUDIO, release 2.0, Accelrys, Parc Club Orsay Universitè 20, Rue Jean Rostand, 91898 Orsay Cedex, France.

Scheme 1

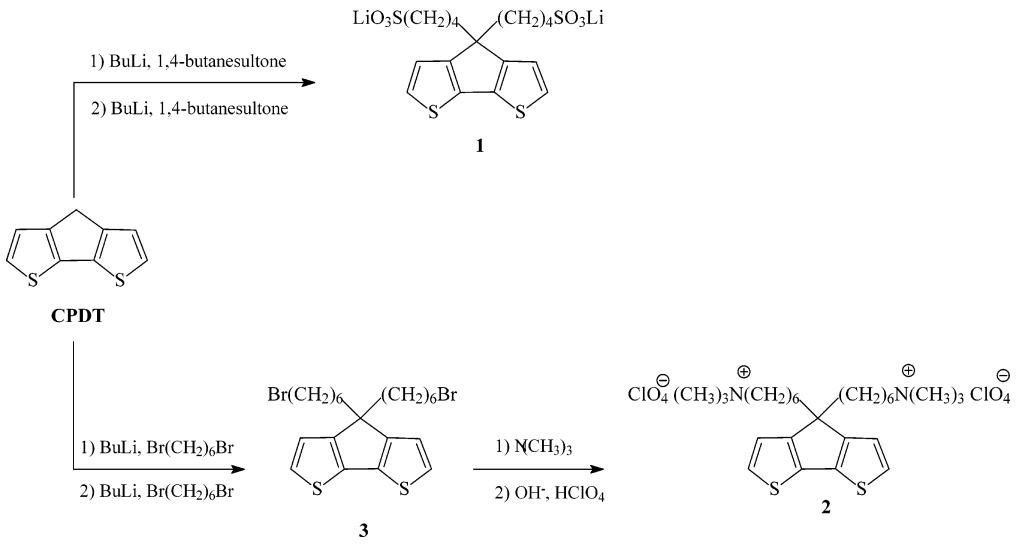

butanesultone and second with another equimolar amount of BuLi and 1,4-butanesultone. Compound **2** was prepared from CPDT through double reaction with BuLi followed by alkylation with 1,6-dibromohexane and nucleophilic substitution with trimethylamine. The obtained dibromide salt **2a** was transformed into the corresponding perchlorate salt **2** by anion exchange and titration of the corresponding hydroxide with perchloric acid.

3.2. Polymer Synthesis and Characterization. *3.2.1. Poly(1) Electrodeposition and Characterization.* The lithium salt of **1** is so sparingly soluble in acetonitrile that polymerization is prevented. Also the Bu_4N^+ salt of the monomer was prepared but it resulted in being scarcely soluble too.

Solubility is obtained by the addition of 2:1 $HClO_4$ to the **1** salt suspension and is due to protonation of the sulfonate moieties. Under these conditions cyclic voltammetry (CV) displays the oxidation peak of the monomer at 0.67 V, that is, the potential value of 4-alkyl-substituted cyclopentadithiophenes.[33]

It must be remarked that with time (some hours) the sulfonic acid form of the monomer is oxidized by air in the acidic medium so that operations must be performed immediately after the acid addition to avoid uncontrolled chemical polymerization in solution.

Potentiostatic oxidation at the peak potential results in the buildup of the polymer on the electrode. The CV of the deposit is shown as a single redox process at $E°$ = ca. 0.0 V (Figure 1a), that is, the same value for the analogous polymer bearing a butyl chain at position 4,[33] providing evidence that the substituent does not influence the redox properties of the polymer chain. The polymer film after dedoping displays a maximum adsorption at 550 nm (Figure 1b), indicating an extensive conjugation length, comparable with that of the alkyl-substituted analogues.[33]

The bulk oxidized polymer produced by oxidative electrolysis (see Experimental Section) is a dark blue material extensively soluble in water (>10 g L^{-1}). The blue-green water solution shows an extended absorption

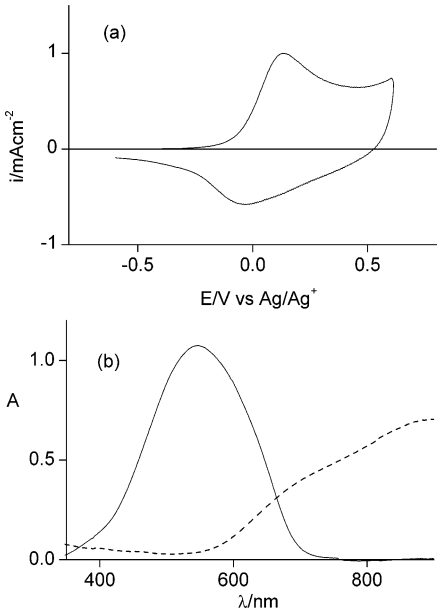

Figure 1. (a) Cyclic voltammetry for poly(1) film in acetonitrile + 0.1 M Bu_4NClO_4. Scan rate: 0.1 V s^{-1}. Reversible charge: 5 mC cm^{-2}. (b) UV−vis spectra of neutral (—) and oxidized (- - -) poly(1) film in acetonitrile + 0.1 M Bu_4NClO_4.

covering the visible range (Figure 2a). Its reduction with hydrazine makes the solution violet with a peak at 560 nm and a shoulder at 630 nm. MALDI-TOF analysis did not give information on the degree of polymerization, DP, which was gained instead by UV−vis data (see next section).

The conductivity of the polymer, cast from 1% solution of the doped form, is 5×10^{-3} S cm^{-1}, that is, considerably lower than that of the corresponding monosulfonate analogue poly4-(4*H*-cyclopentadithien-4-yl)butanesulfonate (0.6 S cm^{-1} [22]). This is attributable to the increase of the interchain distance for hopping produced by disubstitution.[33]

3.2.2. Poly(2) Electrosynthesis and Characterization. The CV of the monomer displays regularly the oxidation peak of the cyclopentadithiophene moiety at 0.70 V. Yet potentiostatic oxidation at the peak does not result in the deposition of the polymer but in its production in solution.

(33) Zotti, G.; Schiavon, G.; Berlin, A.; Pagani, G. *Macromolecules* **1994**, *27*, 1938.

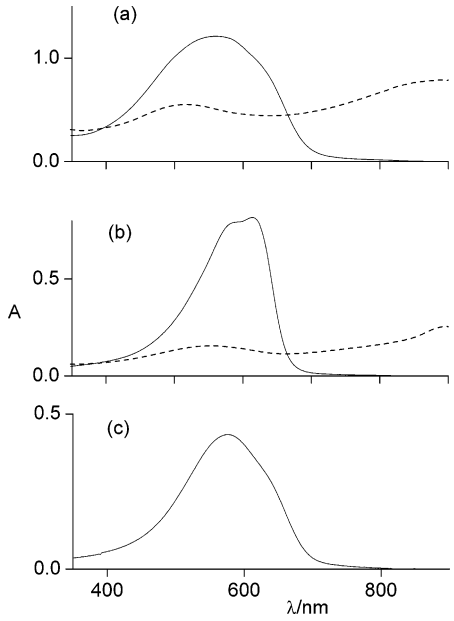

Figure 2. UV−vis spectra of polymer solutions: (a) as-prepared (- - -) and hydrazine-reduced (—) poly(1) in water; (b) as-prepared (- - -) and hydrazine-reduced (—) poly(2) in acetonitrile; (c) poly(2)−OH in water.

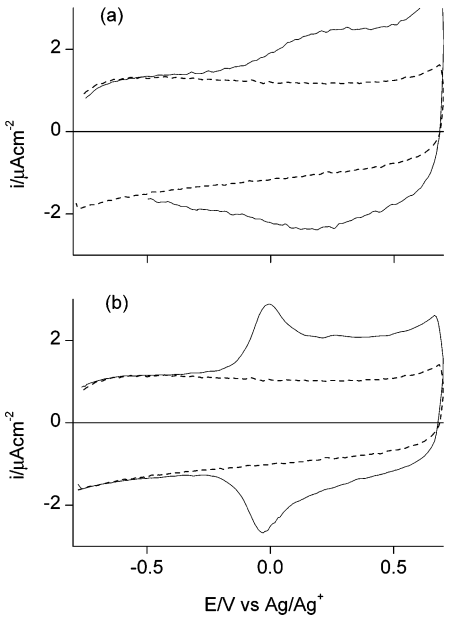

Figure 3. Cyclic voltammograms for (a) poly(1) and (b) poly(**2**) monolayer on bare ITO in acetonitrile + 0.1 M Bu_4NClO_4. Scan rate: 0.1 V s^{-1}.

The polymer is obtained as a blue solution which after hydrazine treatment displays a maximum adsorption at 615 nm with a shoulder at 580 nm (Figure 2b). The spectrum, which is similar to that of poly(cyclopentadithiophene) substituted by a long (octyl or dodecyl) alkyl chain,[33] shows a fine structure indicative of a rigid-rod-shaped polymer chain with extended conjugation length. MALDI-TOF analysis has given a series of oligomeric peaks (M_n-ClO_4, $n = 3-10$) centered at the hexamer ($n = 6$).

Bulk oxidized polymer is produced by oxidative electrolysis of the monomer in acetonitrile (see Experimental Section). The dark blue poly(2)−ClO_4 is insoluble in methylene chloride and acetone but very soluble in acetonitrile (>20 g L^{-1}).

The conductivity of the polymer, cast from 1% solution in acetonitrile, is 7×10^{-3} S cm^{-1}. This value is comparable with that of poly(1), in agreement with the similar structure.

Poly(2)−ClO_4 is converted to the water-soluble hydroxide form poly(2)−OH by anion exchange. Poly(**2**)−OH is obtained in the undoped form, as indicated by the UV−vis spectrum showing a strong band at 575 nm with a shoulder at 630 nm (Figure 2c), similar to that of poly(1) in water (Figure 2a). It is suggested that both the fine structure and the bathochromic shift shown in acetonitrile solution are due to the lower dielectric constant of the solvent which enhances the repulsion between the positively charged terminals and stiffen the molecule in a more planar conformation. The longer wavelength of absorption of poly(2) compared with that of poly(1) (575 vs 560 nm) indicates a slightly lower DP for the latter. In fact, simple calculations using λ_{max} of the monomers (311 nm) allow one to interpolate a DP of ca. 5 for poly(1) vs 6 for poly(2), the latter in agreement with MALDI analysis.

3.3. ESA Layering of Polymers. Layering was performed from the undoped polymers since this form was shown to be more efficient in this respect.[24] Moreover, the poly(1) polyanion may enjoy a charge density higher than that in the oxidized form, which is favorable for the formation of stable layers.[6]

3.3.1. Monolayer Formation. Poly(1) Monolayer. The solution of poly(1) used for the initial layer was brought to pH = 3 with added $HClO_4$. In fact, we found that a high reproducibility is obtained only if the poly(1) solution is acidic. This is attributed to the formation of positively charged sites at the ITO surface, protonated hydroxyl functions being the coordinating sites of the poly(1) monolayer.[34]

The CV of bare ITO after poly(1) treatment (Figure 3a) shows a single and round redox process at $E° = 0.2$ V. The reversible charge Q_r, measured at a switching potential $E_\lambda = 0.7$ V, is 10 μC cm^{-2}. The CV reversible response is perfectly stable to potential cycling.

The UV−vis spectrum of this monolayer (after compensation with hydrazine) shows a clear peak at 560 nm as for the bulk polymer.

Poly(2) Monolayer. The CV of bare ITO after poly(2) treatment (Figure 3b) shows a single sharp redox process at $E° = -0.05$ V, that is, a potential 0.25 V more negative than that of the poly(1) monolayer. This result, which may only partially be attributed to the lower energy gap of poly(2) (2.16 vs 2.21 eV), is mainly due to the opposite sign of the charge on the undoped poly(2) and poly(1) chains. The reversible charge Q_r, measured at a switching potential $E_\lambda = 0.7$ V, is 10 μC cm^{-2}. It is noticeable that the value is the same measured for poly(1), which indicates an identical disposition of the linear rod molecules over the surface. The UV−vis spectrum of the monolayer shows the maximum absorption at 575 nm as for the bulk polymer.

Polycationic (trimethylammonium-substituted) polymers are reported to adsorb on negatively charged sites

(34) Nuesch, F.; Rothberg, L. J.; Forsythe, E. W.; Le, Q. T.; Gao, Y. *Appl. Phys. Lett.* **1999**, *74*, 880.

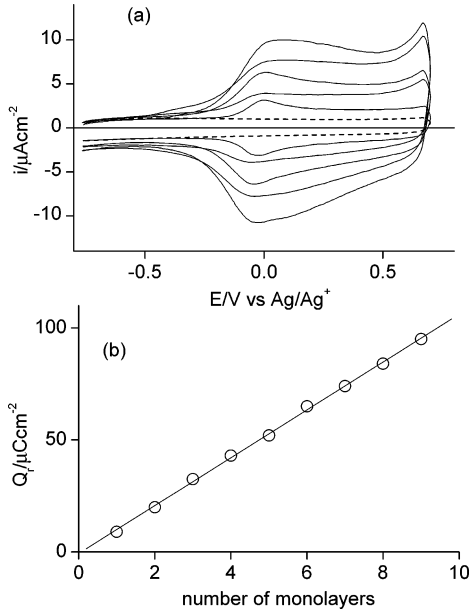

Figure 4. CV of (poly(**2**)/poly(1))$_n$ multilayers on bare ITO in acetonitrile + 0.1 M Bu_4NClO_4: (a) voltammetric responses and (b) reversible charge vs number of monolayers.

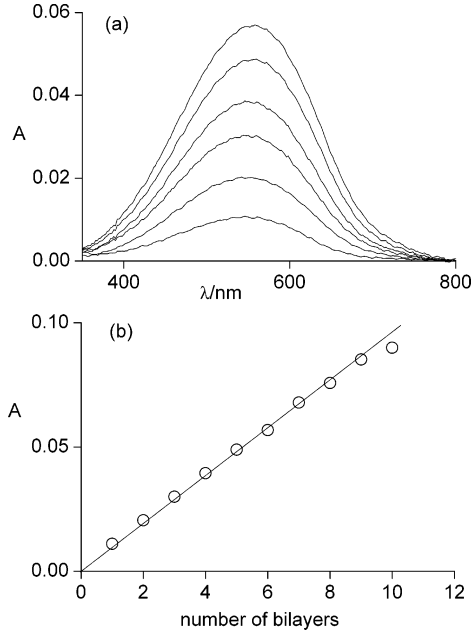

Figure 5. UV−vis spectroscopy of (poly(2)/poly(1))$_n$ multilayers on bare ITO (after hydrazine reduction): (a) spectral prophiles and (b) absorbance vs number of bilayers.

(polysilicic acid chains) of glass.[35] Similarly, the surface of ITO shows negatively charged characteristics due to the presence of dangling In−O^- and Sn−O^- bonds. These are the coordinating sites of poly(2) monolayer.

3.3.2. Multilayer Formation on Bare ITO. In general and like in analogous layers,[24] the CV response of the multilayers described here does not fully develop at the first CV scan but preliminary scanning is required to activate the whole multilayer. Typically samples of 10 bilayers require three CV cycles at 0.02 V s^{-1} to develop their full response.

The CV reversible response is perfectly stable to potential cycling (no loss of electroactivity is observed after at least 25 scans at 0.02 V s^{-1}).

Highly reproducible results were obtained as indicated by the standard error of the reversible charge, which is typically less than 2% for a series of five samples.

The robustness of the multilayers, commonly found in this type of multilayering, was demonstrated by standard sticky-tape tests.

*Poly(**2**)/Poly(**1**) Multilayers.* Poly(2)/poly(1) ESA on bare ITO (Figure 4a) proceeds with linearity as shown by CV charge analysis (10 μC cm^{-2} $monolayer^{-1}$, Figure 4b). It is remarkable that the slope is the same of the charge for the initial layers (ITO/poly(2) and ITO/poly(1), 10 μC cm^{-2}) whereas in general the first monolayer is different from the following ones. Also the spectral analysis (after full reduction) shows that the maximum absorbance at 560 nm increases linearly with the number of dipping cycles up to at least 10 bilayers (Figure 5). The slope is 9×10^{-3} a.u. $bilayer^{-1}$. From this result and using the extinction coefficient ϵ of 1.2×10^4 M^{-1} cm^{-1},[24] the optical coverage degree is ca. 2×10^{-10} mol cm^{-2} $monolayer^{-1}$ (mol as a repeat unit).

In the presence of added electrolyte (NaCl up to 0.5 M concentration) the ESA of poly(2)/poly(1) multilayers is the same as that in its absence, with only a slight increase of the growth rate (10−20% maximum). In conventional ESA, such as PSS/PAH multilayers, the literature reports a rate even 10 times faster in the same electrolyte at a lower (0.1 M) concentration,[31] attributable to polymer chain folding after charge screening. Our result is perfectly in line with the stiffness of the linear polythiophene polymer chains investigated here, which does not allow such morphological changes.

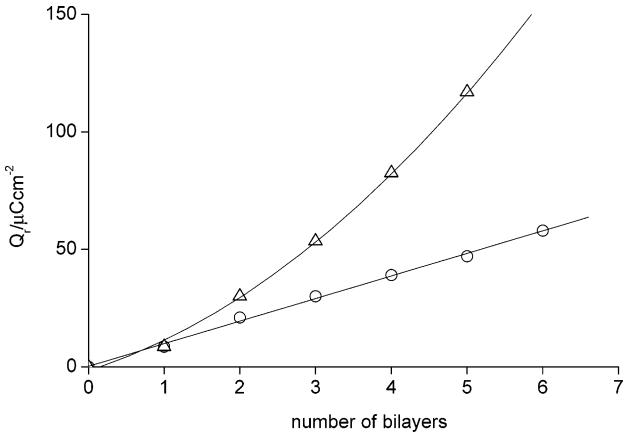

Figure 6. Reversible charge vs number of bilayers for (Δ) poly(**2**)/PVS and (O) poly(**2**)/PSS multilayers on bare ITO in acetonitrile + 0.1 M Bu_4NClO_4.

Poly(2)/PSS; Poly(2)/PVS; Poly(1)/PAH and Poly(1)/PDDA Multilayers. Poly(**2**)/PSS multilayering was performed on bare ITO/glass electrodes starting from a poly(2) monolayer. The charge growth is linear (Figure 6) with a slope of 10 μC cm^{-2} $bilayer^{-1}$, that is, the same value of the initial monolayer. At difference the formation of (poly(2)/PVS)*n*, performed similarly, proceeds with a supralinear character (Figure 6) following a linear dependence of the reversible charge with $n^{1.5}$.

Analogous responses were obtained with poly(1) using PAH or PDDA. ESA of poly(1)/PAH proceeds linearly

(35) Poptoshev, E.; Claesson, P. M. *Langmuir* **2002**, *18*, 1184.

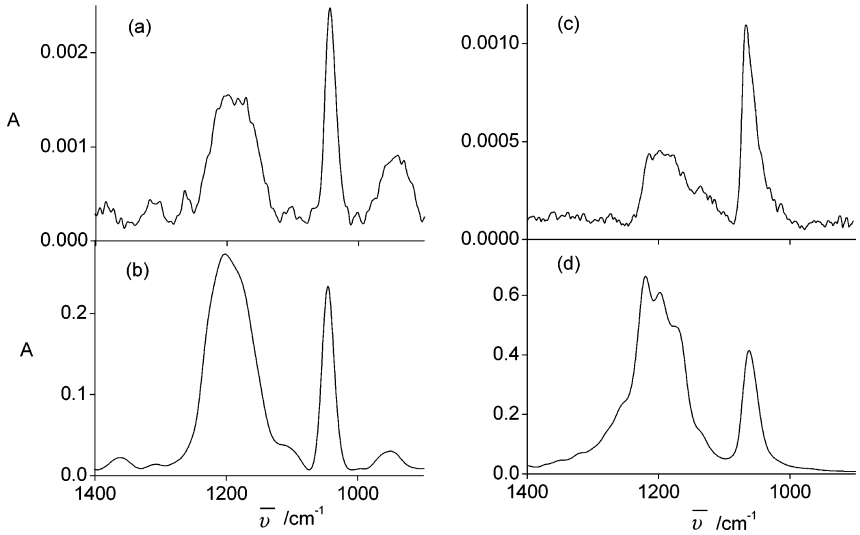

Figure 7. FTIR spectra of (a) Au/MEA/poly(1) monolayer and (b) bulk poly(1) ammonium salt; (c) Au/MPS monolayer and (d) bulk MPS.

up to at least 10 poly(1)/PAH bilayers with an increase (10 μC cm^{-2} bilayer^{-1}) equal to the amount of the first layer (10 μC cm^{-2}), which indicates a very regular deposition. With poly(1)/PDDA the layering starts with the same amount of the first layer but proceeds supralinearly (linearly with $n^{1.4}$).

A supralinear growth indicates a progressive roughening of the deposit produced by loops and ends.[36] It is likely that if the linear-charge density of the polymer chains do not match each other, such loops and chain ends are favored and a progressively disordered structure is produced.

3.4. Mono- and Multilayering on ATS-Primed ITO. Poly(1) and poly(2) were adsorbed on ATS-primed (positively charged) and ATS/PSS-primed (negatively charged) ITO/glass electrode, respectively. The produced monolayer gives a CV signal at the same redox potential of the layer on bare ITO but with a higher coverage (Q_r = 20−30 μC cm^{-2}). A higher coverage on ATS-primed ITO compared with the bare substrate is a general feature for the investigated layers and reflects an expected degree of disorder (cross-links) in the structure of the underlying ATS layer. Some degree of polymerization frequently occurs with trimethoxysilanes due to traces of moisture.[37]

These values are about half of those previously measured for monosubstituted polymer analogues,[24] which may be attributed to the higher steric hindrance of the actually investigated repeat units.

Alternating poly(1)/poly(2) on ATS-primed and poly(2)/PSS on ATS/PSS-primed ITO/glass electrodes proceeds regularly. The growth is linear but, as expected, with a higher slope (e.g., 15 μC cm^{-2} bilayer^{-1} for poly(2)/PSS) than on bare ITO.

3.5. Mono- and Multilayering on Primed Gold. CV analysis of poly(1)/poly(2) ESA on MEA-primed gold shows that the growth proceeds with linearity (10 μC cm^{-2} monolayer^{-1}) up to at least 10 monolayers. Also in this case the charge for the first layer is the same of the slope (ca. 10 μC cm^{-2}). Similar results were obtained from MPS-primed gold with poly(2)/poly(1) alternation.

3.6. IRRAS Spectroscopy of Monolayers on Gold. The FTIR spectrum of poly(1) is dominated by strong bands at 1200 and 1050 cm^{-1} due to the antisymmetrical (A) and symmetrical (S) stretching modes of the sulfonate moieties. These bands exhibit a transition dipole moment oriented perpendicular and parallel to the alkyl chain axis, respectively, and are therefore useful for a determination of the molecular orientation of the polymer layers to the electrode plane by using the so-called surface selection rule for IR spectroscopy at metal surfaces.[38]

The IRRAS spectrum of a Au/MEA/poly(1) monolayer is shown in Figure 7a together with the bulk spectrum recorded for poly(1) (produced by compensation of the polymer film with hydrazine) as KBr pellet (Figure 7b). The comparison indicates a marked decrease of the intensity of A relative to S in the monolayer. The same is observed in a monolayer of MPS on gold compared with bulk MPS (Figure 7c,d) and provides evidence for an upward orientation of the sulfonate moieties from the gold surface.[39]

3.7. XRD Analysis of Multilayers. XRD measurements in Bragg−Brentano geometry have shown to be suitable to evidence order in ultrathin (5 nm) organic films.[40] Hence, if applied to the multilayers reported here, they can shown coherent diffraction effects corresponding to interlayer spacings.

(Poly(1)/PAH)$_{10}$, (poly(2)/PSS)$_{10}$, and (poly(1)/poly(2))$_{20}$ on ITO/glass were investigated. The overall aspect of the spectra indicated a very poor order degree. Only in the case of (poly(1)/PAH)$_{10}$ is a clear sharp peak detected on the background at $2\theta = 8.7°$ (see Figure 8), for which the corresponding spacing is equal to 1.015 nm. Line profile analysis gave indication of complete

(36) Lavalle, Ph.; Gergely, C.; Cuisinier, F. J. G.; Decher, G.; Schaaf, P.; Voegel, J. C.; Picart, C. *Macromolecules* **2002**, *35*, 4458.
(37) (a) Fadeev, A. Y.; McCarthy, T. J. *Langmuir* **2000**, *16*, 7268. (b) Ulman, A. in *An introduction to ultrathin organic films*: *from Langmuir-Blodgett to self-assembly*; Academic Press: Boston, 1991. (c) Ulman, A. *Chem. Rev.* **1996**, *96*, 1533.
(38) Arnold, R.; Terfort, A; Woll, C. *Langmuir* **2001**, *17*, 4980.
(39) Bonazzola, C.; Calvo, E. J.; Nart, F. C. *Langmuir* **2003**, *19*, 5279.
(40) Botta, C.; Destri, S.; Porzio, W.; Sassella, A.; Borghesi, A.; Tubino, R. *Opt. Mater.* **1999**, *12*, 301.

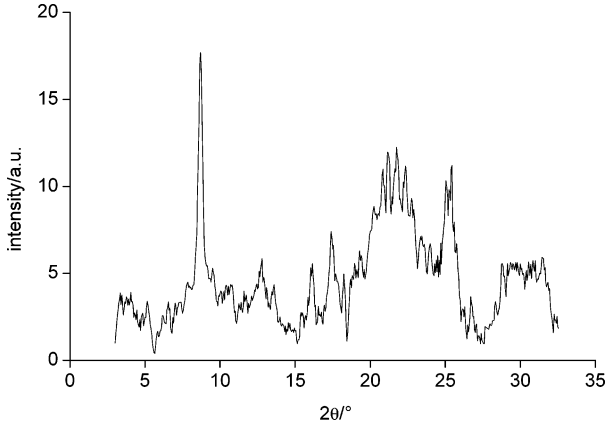

Figure 8. XRD patterns of $(poly(1)/PAH))_{10}$ multilayer on bare ITO.

coherence along the film thickness (<15 nm).[41] Grazing incidence diffraction experiments performed on the same sample to increase the signal-to-background ratio gave no further indication. Molecular modeling using MATSTUDIO program package[32] allowed for a series of minimized models where the repetition of SO_3^- groups, which supply a major contribution to the diffraction, can vary from 0.95 up to over 1.2 nm. It should be emphasized that PAH molecules (the blue molecules shown in Figure 9) may assume different conformations, yielding various repetitions.

One of the models displaying the lower energy is reported in Figure 9. The top view A shows a repetition close to 1.02 nm, a value in full agreement with the experimental observations.

It should be mentioned that, to the best of our knowledge, this result is the first ever obtained for self-assembled two-component $(A/B)_n$ polyelectrolyte multilayers. In fact, only X-ray reflectivity (XRR) data appeared recently on ionenes giving, besides the overall film thickness and roughness, Bragg reflections due to the ionene internal structure, but a definite interlayer spacing, detectable with wide angle (WA) XRD, was not reported.[42]

Moreover, the detection of XRD peaks in only one of the multilayers is not an unusual outcome. In a recent paper on ESA of several types of polycationic (mainly ionenes) and polyanionic polymers, with various linear charge densities and different tendencies to give ordered phases,[43] it was found that the realization of ordered ESA structures is not the straigtforward result of the ordering ability of the single components.

3.8. Atomic Force Microscopy Analysis of Multilayers. We have imaged and compared the surfaces of $(poly(1)/PAH)_{10}$, $(poly(2)/PSS)_{10}$, and $(poly(1)/poly(2))_{20}$ multilayers on the float glass surface.

Topographic images of $2 \times 2\ \mu m^2$ dimension have been taken. The bare glass substrate is rather flat with a roughness of ca. 0.7 nm. The surface morphology and roughness of the multilayers is increased moderately to 1 nm for $(poly(1)/PAH)_{10}$ and to 2 nm for $(poly(2)/PSS)_{10}$ and $(poly(1)/poly(2))_{20}$.

AFM was used also for the direct measurement of polymer film thickness. The AFM probe tip itself was used to remove a portion of the film so as to expose the substrate. The height of the film above the substrate was obtained directly via cross-section analysis.[44]

Height drops of ca. 10 nm could be measured for $(poly(1)/PAH)_{10}$ and $(poly(2)/PSS)_{10}$ samples in agreement with the value calculated from line profile analysis of XRD patterns.

3.9. The Layer Structure. *3.9.1. The Monolayer.* EQCM analysis has allowed evaluation of the electron stoichiometry for oxidation of cyclopentadithiophene-based polymers (one electron per repeat unit at $E_\lambda = 0.7$ V[24]). Thus, the charge stored at the poly(1) and poly(2) monolayers (10 μC cm^{-2}) indicates a coverage degree of 1×10^{-10} mol cm^{-2}. This value is in appreciable agreement with the spectrophotometric value of 2×10^{-10} mol cm^{-2} monolayer^{-1} obtained from poly(2)/poly(1) bilayers (see above).

The area calculated for **1** in different conformations of the alkyl chains is between 0.6 and 0.8 nm^2, corresponding to a coverage degree of $2.1-2.8 \times 10^{-10}$ mol cm^{-2}. Thus, it results that the poly(cyclopentadithiophene) monolayers engage about half of the available surface.

The monolayer has the same coverage degree independently of the charge sign (poly(1) or poly(2)) and of the substrate (ITO or MEA-primed gold) given a sufficient surface charge density is present. This result is clearly allowed by the high charge density present in the polymers. Though information on the disposition (parallel or perpendicular) of the polythiophene plane on the surface could not be obtained, the IRRAS spectra indicate that the polythiophene rigid rods lay on the surface with the alkyl chains oriented upward.

3.9.2. The Multilayer. The regularity of the first monolayer is known to determine in general the regularity of the subsequent multilayering but this is not the case for electrostatic self-assembly.[6] More important appears to be the selection of the polyion pair constituting the bilayer which determines the degree of charge compensation as a function of either (a) the relative charge densities of the components or (b) the charge density matching.

Polymer charge density is known to affect the characteristics of the adsorbed layer on mica so that the layer becomes more thin and flat as the charge density is increased.[45] More complex and under discussion is the role of the polymer charge density in the ESA process.[6,46] Charge density matching has been considered in a certain number of cases[6] and mismatch has been retained responsible for the positive or negative deviations from linearity in the growth rate (deposited mass vs number of deposition cycles).[6]

The ESA growth of the investigated multilayers was found to be linear with poly(1)/poly(2), which is not unexpected since charge density matching is obvious.

(41) Enzo, S.; Fagherazzi, G.; Benedetti, A.; Polizzi, S. *J. Appl. Crystallogr.* **1988**, *21*, 536.
(42) Arys, X.; Laschewsky, A.; Jonas, A. M. *Macromolecules* **2001**, *34*, 3318.
(43) Arys, X.; Fischer, P.; Jonas, A. M.; Koetse, M. M.; Laschewsky, A.; Legras, R.; Wischerhoff, E. *J. Am. Chem. Soc.* **2003**, *125*, 1859.
(44) McAloney, R. A.; Sinyor, M.; Dudnik, V.; Goh, M. C. *Langmuir* **2001**, *17*, 6655.
(45) Rojas, O. J.; Ernstsson, M.; Neuman, R. D.; Claesson, P. M. *Langmuir* **2002**, *18*, 1604.
(46) Schoeler, B.; Kumaraswamy, G.; Caruso, F. *Macromolecules* **2002**, *35*, 889 and references therein.

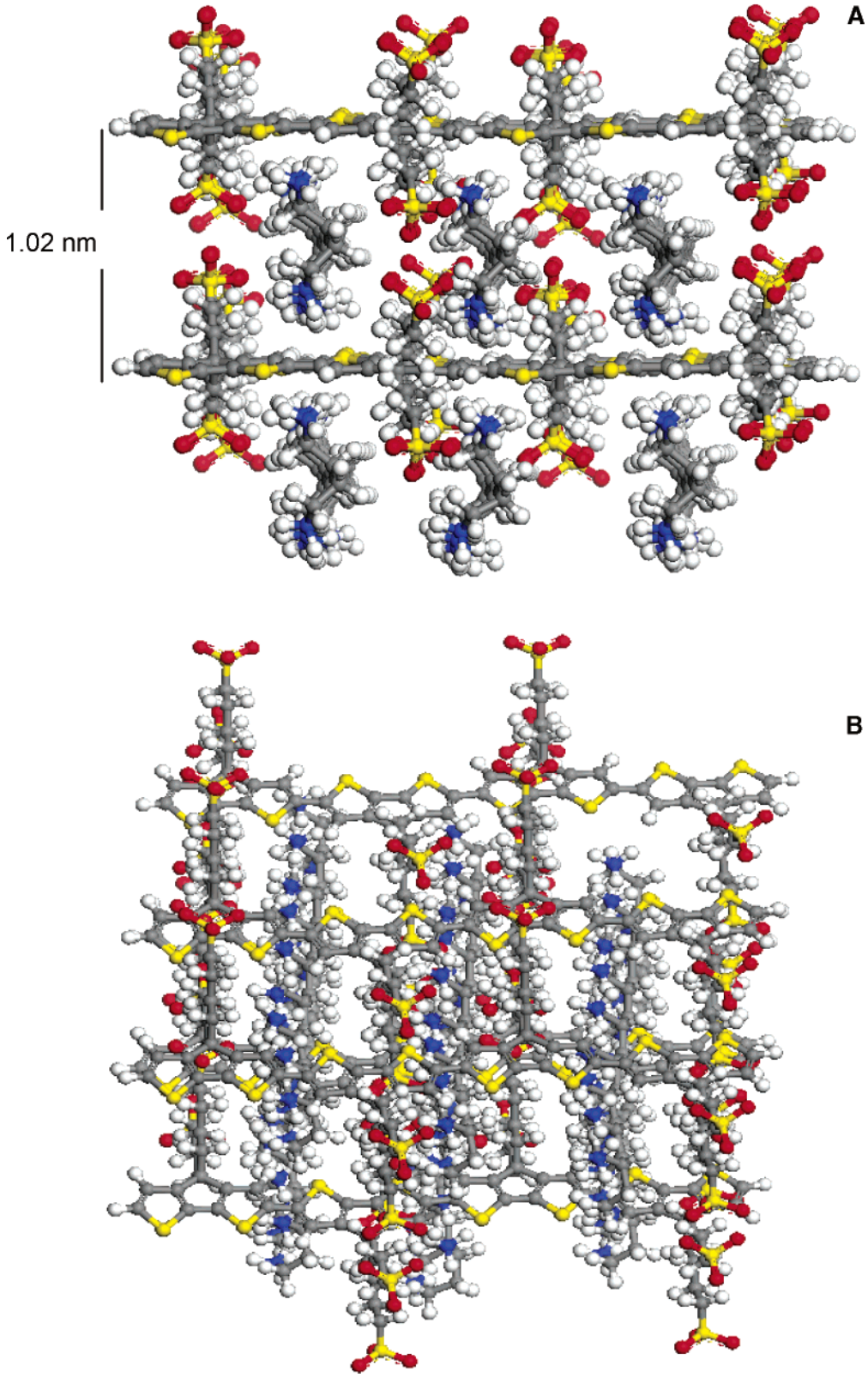

Figure 9. Model of (poly(**1**)/PAH)$_{10}$ as viewed parallel to the growth axis (A) and along the PAH chains (B), ortho-normal to the previous one.

Differences were found in the mixed multilayers since poly(1)/PAH and poly(2)/PSS grow regularly whereas poly(1)/PDDA and poly(2)/PVS are disordered. It appears that PAH and PSS matches the polythiophene chain better, a higher (PVS) or lower (PDDA) charge density bringing about a significant deviation from regularity.

The case of poly(1)/PAH is particularly interesting since the low roughness increase over that of the substrate is accompanied by the display of XRD interference. It appears that in this case the conditions of regular ESA are fulfilled at the maximum degree. It must be remembered that this is the first reported example of interlayer WA-XRD spacing in ESA multilayers.

Finally, it must be noted as an unprecedented result that poly(1)/poly(2) multilayers grow without any effect of ionic strength. This behavior is a clear indication that no effective interchain penetration occurs between adjacent polymer layers, as expected from the stiffness of rigid-rod polythiophene chains.

Conclusions

New water-soluble polycationic and polyanionic polythiophenes with high symmetry and conjugation have been prepared by anodic coupling. The polymers form stable and dense monolayers on bare indium−tin−oxide and primed-gold surfaces. Electrostatic self-assembly of multilayers from these polymers occurs with regularity on the preformed monolayers. Films with a minimal interchain penetration are obtained from the polythiophenes due to chain stiffness. IRRAS and XRD analysis have evidenced in these ESA layers a degree of order not observed in previous polyconjugated multilayers and likely due to a good geometrical matching between anionic and cationic polymers via proper charge density values.

These results are promising for the development of polymer-based, nanometer-scale 2D structures with anisotropic electronic (optical and conductive) properties.

Acknowledgment. The authors would like to thank A. Randi and S. Sitran of the CNR for their technical assistance. We are also indebted to MIUR-FIRB (project code RBNE019H9K).

CM0351644